Activated carbon xerogels for the removal of the anionic azo dyes Orange II and Chromotrope 2R by adsorption and catalytic wet peroxide oxidation

Rui S. Ribeiro, Nady A. Fathy, Amina A. Attia, Adrián M.T. Silva, Joaquim L. Faria, Helder T. Gomes

PII: S1385-8947(12)00527-X
DOI: http://dx.doi.org/10.1016/j.cej.2012.04.065
Reference: CEJ 9196

To appear in: *Chemical Engineering Journal*

Received Date: 10 January 2012
Revised Date: 21 April 2012
Accepted Date: 23 April 2012

Please cite this article as: R.S. Ribeiro, N.A. Fathy, A.A. Attia, A.M.T. Silva, J.L. Faria, H.T. Gomes, Activated carbon xerogels for the removal of the anionic azo dyes Orange II and Chromotrope 2R by adsorption and catalytic wet peroxide oxidation, *Chemical Engineering Journal* (2012), doi: http://dx.doi.org/10.1016/j.cej.2012.04.065

Activated carbon xerogels for the removal of the anionic azo dyes Orange II and Chromotrope 2R by adsorption and catalytic wet peroxide oxidation

Rui S. Ribeiro[a], Nady A. Fathy[b], Amina A. Attia[b], Adrián M.T. Silva[c], Joaquim L. Faria[c], Helder T. Gomes[a,c,*]

[a] *Department of Chemical and Biological Engineering, School of Technology and Management, Polytechnic Institute of Bragança, Campus de Santa Apolónia, 5300-857 Bragança, Portugal.*

[b] *Surface Chemistry and Catalysis Laboratory, National Research Centre, 12622 Dokki, Cairo, Egypt.*

[c] *LCM - Laboratory of Catalysis and Materials - Associate Laboratory LSRE/LCM, Faculdade de Engenharia, Universidade do Porto, Rua Dr. Roberto Frias, 4200-465 Porto, Portugal.*

*Corresponding author. Tel.: +351 273 303 110; Fax: +351 273 313 051.

E-mail address: htgomes@ipb.pt

Abstract

Activated carbon xerogels (ACXs) were tested for the removal of azo dyes in aqueous solutions, either by adsorption or by catalytic wet peroxide oxidation (CWPO). Two azo dyes, Orange II (OII) and Chromotrope 2R (C2R), were chosen as model pollutants. The ACXs were produced by activation of an organic resorcinol-formaldehyde xerogel (RFX). Three different activation procedures were carried out producing five distinct ACXs: steam at 1073 K (ACX-S), chemical impregnation with H_3PO_4 at 773 K (ACX-P) and alkali activation with dry KOH at 973 K (ACX-K), using three different mass ratios of KOH/RFX, namely 1:1 (ACX-K1), 2:1 (ACX-K2) and 4:1 (ACX-K4).

The results obtained in the adsorption experiments carried out at pH = 3, T = 303 K, adsorbent load of 0.1 g L^{-1} and azo dye concentration of 100 mg L^{-1} show that the interaction between the carbon materials and the anionic dyes is enhanced with the basicity of the carbon surfaces. ACX-K materials, the carbon materials with higher basicity amongst those prepared, exhibit high adsorption performances for the removal of both dyes, namely from over 215 mg g^{-1} (for adsorption of C2R on ACX-K2 after 150 min) up to 499 mg g^{-1} (for adsorption of OII on ACX-K4 at the same period of time). Furthermore, with ACX-K materials in CWPO (*i.e.*, using H_2O_2) increments in the removal of C2R as high as 33 %, 24 % and 20 %, in comparison to the removals obtained by adsorption, where obtained when ACX-K1, ACX-K2 and ACX-K4 were respectively tested at 303 K. Increasing the operating temperature (T = 323 K), the removal increments achieved by CWPO, compared to the removals obtained by adsorption at the same temperature, increase 67 %, 59 % and 49 %, when ACX-K1, ACX-K2 and ACX-K4 were respectively tested. Recycling studies with ACX-K1 puts in evidence the

high stability of this catalyst in CWPO, since it was observed, after a first reaction run, that the catalytic activity of this material is not affected by its successive reuse.

Increasing the operating temperature (T = 323 K) and the adsorbent load (0.5 g L^{-1}), ACX-K4 is able to completely remove the C2R content by adsorption. In the case of ACX-K1 and ACX-K2, adsorption removals over 97 % of the C2R content are attainable.

Keywords: Activated carbon xerogel; Activation procedures; Basic character; Catalytic wet peroxide oxidation (CWPO); Azo dyes.

1. Introduction

The presence of dyes in textile effluents impart to the receiving water streams strong colourations and are readily associated to high environmental and social problems. The development of treatment technologies, which can be efficient on the removal of colour from wastewater, is thus an important challenge.

Activated carbons (ACs) are widely used as adsorbents in a variety of processes for water purification. It is also known that hydrogen peroxide (H_2O_2) can be decomposed to O_2 and H_2O, or towards $OH^{\bullet}$ radicals, over suitable solid catalysts. These radicals are able to oxidize organic pollutants to carbon dioxide and water, as a consequence of their high oxidant potential [1]. It has been previously shown that, in the presence of H_2O_2, ACs without any metal added can act as catalysts for the Catalytic Wet Peroxide Oxidation (CWPO) process to treat organic pollutants in aqueous solutions [2-5]. At the same time, the unique porous structure and conducting networks revealed by carbon gels, viz carbon aerogels (CAs), carbon cryogels (CCs) or carbon xerogels (CXs), have attracted significant interest in the search of new applications for these porous carbon materials.

The preparation of carbon xerogels from organic resorcinol–formaldehyde xerogels was first reported in 1989 by Pekala [6]; however, studies on this subject have been widely performed only in recent years [7-9], exploring their use in many applications such as adsorbents [10, 11], catalysts [12] and electrodes [13]. Recently, carbon xerogels have also proved to be excellent alternatives to activated carbons in various processes [14-16]. These materials are composed of microporous interconnected sphere-like nodules, formed during the gel synthesis *via* a microphase separation mechanism induced by polymer growth [17]. The

size of these nodules is mainly regulated by the synthesis pH [18]. As a result, the size of the voids between the nodules after drying and pyrolysis, and thus the meso- or macroporosity of the final carbon material, is also regulated: it depends on both the composition of the precursor solution (pH, mainly) and the drying procedure [18]. For specific applications, and despite their higher cost compared with activated carbons, carbon xerogels are interesting since the accurate tailoring of the pore texture allows to increase significantly the performance of catalytic and electrocatalytic processes and enable their application to dynamic adsorption. For example, Girgis *et al.* [11] studied the methylene blue (MB) adsorption capacity of a series of carbon xerogels synthesised from resorcinol-formaldehyde resins pyrolyzed at a temperature ranging from 773 K to 973 K. The results showed a good MB adsorption capacity (222 mg g^{-1}) for the carbon xerogel pyrolyzed at 973 K, which displayed a specific surface area of 735 m^2 g^{-1}. However, in order to increase the adsorption capacity, the relatively low inner surface area of carbon xerogels (≈700 m^2 g^{-1}) must be developed, for example, by chemical or physical activation. Resorcinol-formaldehyde resins appear in this way as promising raw materials for the production of ACXs with a highly-developed porosity and surface area due to the following reasons: the considerably high fixed-carbon content, high inherent porosity, controllable macropore and micropore structure and relatively low price of the reagents [19].

In the present work, searching new applications, different ACX materials were synthesised and tested for the removal of azo dyes in aqueous solutions, either by adsorption or by CWPO. Two azo dyes were chosen as model pollutants – Orange II (OII) and Chromotrope 2R (C2R) – due to their anionic character and their extensive use in the textile industry, as well as in some limited medical diagnosis applications. The ACX materials were produced by activation of an organic xerogel synthesised by polycondensation of resorcinol with

formaldehyde, *i.e*. organic resorcinol–formaldehyde xerogels (RFX). Three different one-stage activation procedures were carried out, producing five distinct ACXs: steam at 1073 K (ACX-S), chemical impregnation with H_3PO_4 at 773 K (ACX-P) and alkali activation with dry KOH at 973 K (ACX-K). For the later, three different mass ratios of KOH/RFX were used, namely 1:1 (ACX-K1), 2:1 (ACX-K2) and 4:1 (ACX-K4).

2. Materials and methods

2.1. Chemicals

Chromotrope 2R ($C_{16}H_{10}N_2Na_2O_8S_2$, Mr 468.39 [CAS number: 4197-07-3], Colour Index Acid Red 29), with molecular structure shown in Figure 1a, was obtained from Fluka. Orange II ($C_{16}H_{11}N_2NaO_4S$, Mr 350.32 [CAS number: 633-96-5], Colour Index Acid Orange 7), with molecular structure shown in Figure 1b, was obtained from Acros Organics. H_2O_2 (30 %, w/v) and sodium hydroxide (98 wt. %) were obtained from Panreac, while sulphuric acid (95–97 wt. %) was obtained from Fluka. Ortho phosphoric acid (85 wt. %) was obtained from Rasayan (Turkey). All chemicals were used as received without further purification. Distilled water was used throughout the work.

FIGURE 1

2.2. Preparation of the organic resorcinol-formaldehyde xerogel (RFX)

RFX was synthesised by a sol-gel procedure. Calculated amounts of resorcinol (R) and sodium carbonate catalyst (C) were dissolved in distilled water, with the molar ratio R/C set at 50. Formaldehyde was added in the molar ratio R/F = 0.5, forming the sol mixture. This mixture was magnetically stirred and the temperature was raised to 353 K, being kept for 30 min in order to homogenise the solution and initiate the polymerization/polycondensation

reactions. The sol was left at room temperature for 24 h to undergo gelling and ageing. The produced aquagel was heated slowly to 333 K and held for 2 h, being finally heated to 383 K for another 2 h to get the organic xerogel, or resin RFX.

2.3. Preparation of activated carbon xerogels (ACX)

Five types of ACXs were obtained by application of three single-step activation procedures on the parent organic RFX (particle size of 0.1 mm), prepared as previously described elsewhere [20]. The first scheme, steam-activation, was performed by slowly heating the powdered organic gel to 623 K, in a stainless steel reactor, introduced in a tube furnace under its own pressure and atmosphere. Steam (generated in a side setup) was admitted and the temperature was slowly increased (10 K min^{-1}) to 1073 K, being kept for 1 h, and then cooled to room temperature. This sample was denoted as ACX-S.

The second activation scheme involved chemical impregnation of the RFX with 85 wt. % H_3PO_4 (without dilution), followed by pyrolysis at 773 K for 90 min, under its own atmosphere. The heating rate was 10 K min^{-1}. The cooled mass was thoroughly washed and the product denoted as ACX-P.

In the third scheme, the organic RFX was subjected to alkali activation with KOH followed by pyrolysis at 973 K for 1 h. Powdered RFX samples were mixed with dry KOH, in successively increasing mass ratios of KOH/RFX (ACX-K) corresponding to 1:1, 2:1 and 4:1. The heating rate was also 10 K min^{-1}. The samples were thoroughly washed and denoted as ACX-K1, ACX-K2 and ACX-K4, respectively. In all preparation schemes, the cooling rate was controlled according to the decrease in atmosphere temperature inside the tube furnace. The chemically-activated carbon xerogels were subjected to thorough washing with distilled water to neutral filtrate, and finally dried overnight in an air oven at 383 K. All carbon

materials were subjected to determination of slurry pH (pH_{slurry}), elemental chemical analysis and carbon yield (Table 1).

2.4. Chemical and textural characterization

The slurry pH for each ACX (pH_{slurry}) was determined by contacting 0.1 g of sample with 100 mL of distilled water, shaken well for 5 min, left the suspension overnight in stoppered bottles and measuring the pH of the supernatant liquid. Elemental analysis was carried out by combustion at 1423 K, in a analytical apparatus (Elementar Vario EL), being the products (H_2O and CO_2) determined by a thermal conductivity detector. The content of oxygen was determined by difference as follows: 100 − % (C+H). FTIR spectra was recorded within the wavenumber range 4000 to 400 cm^{-1} in a spectrometer FTIR-2000 Perkin Elmer, USA.

The porous characteristics of the developed materials were determined by N_2 adsorption at 77 K, using an automatic volumetric apparatus (Gemini 2375, V3.03 Instrument Micrometrics). The samples were primarily degassed overnight at 523 K under a vacuum of 10^{-5} Torr to constant pressure for 2 h, before carrying the adsorption measurements. The specific surface area (S_{BET}, $m^2\ g^{-1}$) was calculated by applying the BET equation to the adsorption data (p/p_0= 0.05 – 0.35) and the total pore volume (V_P) evaluated from the volume of N_2 (as liquid) held at p/p_0 = 0.95. The average pore width (R_p/nm) was calculated from $(2V_{tot}/S_{BET}) \times 10^4$. N_2 adsorption isotherms were also analyzed by means of the α_s-method [21]. By plotting the standard data of α_s-values against adsorbed amount of N_2 ($V_a/cm^3\ g^{-1}$), three texture parameters could be obtained as follows: (1) the total surface area (S^{α}_t) from the slope of the first linear section connecting the adsorption points to origin, (2) the non-microporous surface area (S^{α}_n) from the slope of the rectilinear section connecting the later points (at $\alpha_s \geq 1.0$) and (3) the micropore volume (V^{α}_o) from the intersection of the latter line

extrapolated to meet the V_a-axis (converted into cm^3 of liquid nitrogen). Two other parameters are deduced: microporous surface area (S_{mic}) = $S^{\alpha}_{t} - S^{\alpha}_{n}$, and mesopore volume ($V_{mes}$) = $V_P - V^{\alpha}_{o}$, assuming negligible volume due to macropores.

2.5. Adsorption and reaction experimental procedures

Batch experiments were performed in a 500 mL well-stirred (200 rpm) glass reactor, equipped with a condenser, a temperature measurement thermocouple, a pH measurement electrode and a sample collection port. The reactor was loaded with 250 mL of 100 mg L^{-1} azo dye solution and heated by immersion in a water bath monitored by a temperature controller. Upon stabilization at the desired temperature, the solution pH was adjusted to 3 by means of 1.0 mol L^{-1} H_2SO_4. All experiments were conducted during 150 min, being the typical conditions: T = 303 K, pH = 3 and adsorbent/catalyst load = 0.1 g L^{-1}. A higher temperature (T = 323 K) and a higher adsorbent load (0.5 g L^{-1}) at the higher temperature were parameters also explored in these experiments.

Selected experiments were performed in triplicate, in order to assess reproducibility and error of the experimental results. It was found that the confidence interval was never superior to 2 %, considering 99 % certainty.

2.5.1. Adsorption experiments

In the adsorption runs, the accurate adsorbent amount was added after pH adjustment, in order to reach the desired adsorbent load in solution and define this instant as t_0 = 0 min.

2.5.2. CWPO experiments

In the CWPO runs, a calculated volume of H_2O_2 (6 wt. %) was injected into the system after catalyst addition, in order to reach the desired concentration of 34.6 mmol L^{-1} (corresponding to approximately five and three times the stoichiometric amount needed to completely mineralise C2R and OII, respectively), being that moment considered as t_0 = 0 min. Blank experiments, without any catalyst, were also carried out to assess possible non-catalytic oxidation promoted by H_2O_2.

2.5.3. Hydrogen peroxide decomposition experiments

H_2O_2 decomposition tests were performed considering the same conditions as in the CWPO experiments, except in what concerns to the azo dye solution which was substituted in this case by a correspondent amount of distilled water.

2.6. Analytical methods

Either in adsorption as in CWPO runs, the decolourization was followed by periodic withdrawal of small aliquots (≈ 5 mL), further analysed for azo dye concentration by UV-vis spectrophotometry (Jasco V530). The maximum absorbance of C2R was found in previous works at 509 nm wavelength [3, 4], while the maximum absorbance of OII was found at 486 nm wavelength [22].

The H_2O_2 concentration in decomposition tests was followed by permanganometry [23], through the periodic withdrawal of small aliquots (≈ 5 mL) as in other experiments. In order to separate the solid phase and avoid possible interferences, all samples were subjected to centrifugation at 13 500 rpm during 1 min before analysis.

2.7. Adsorption dynamics

Although a detailed kinetic analysis is not our purpose, the Ho and McKay's pseudo second order model [24] was used in order to evaluate adsorption dynamics, through fitting of the model to the experimental data. The adsorption dynamics described by this model is given in Eq.1, where k_{PSO} is the rate constant of adsorption (g mg^{-1} min^{-1}), q_e is the amount of dye adsorbed at equilibrium (mg g^{-1}) and q_t is the amount of dye on the surface of the adsorbent at any time t (mg g^{-1}). Integrating Eq. 1 for the boundary conditions, *i.e.*, considering $t = 0$ to $t = t$ and $q_t = 0$ to $q_t = q_t$, and rearranging, the linear form given in Eq. 2 is obtained. The constants can be determined by plotting t/q_t against t.

$$\frac{dq_t}{dt} = k_{PSO} (q_e - q_t)^2 \qquad \text{(Eq. 1)}$$

$$\frac{t}{q_t} = \frac{1}{k\, q_e^2} + \frac{1}{q_e} t \qquad \text{(Eq. 2)}$$

3. Results and discussion

3.1. General physical-chemical properties of the prepared ACXs

Table 1 shows the general characteristics of the prepared ACXs under different activation processes. The characterization of the RFX resin is also included for comparison purposes. The elemental analysis of RFX show a chemical composition of C = 58.4 %, H = 4.7 % and O = 36.9 %, which corresponds to H/C and O/C ratios of 0.97 and 0.47, respectively, proving that small amounts of H and O are released through the H_2O formation reaction. Regarding the synthesis of the ACXs, it is observed that the carbon yield varies between 11.0 %

(ACX-K1) and 30.5 % (ACX-P). In addition, after the activations, the composition of C increases considerably, while H and O decrease. It is well established that pyrolysis, particularly of carbonaceous materials, decomposes the functional groups containing heteroatoms, which are released in the form of small compounds (alcohols, ethers, ketoses, acids and water) and thus enrich the carbon content (*cf*. Table 1, C from 58.4 % to around 83.3 %). On the other hand, hydrogen and oxygen are accordingly reduced from 4.7 % down to 2.1 % and from 36.9 % down to 13.4 %, respectively.

It is interesting to note that in the series of KOH activated xerogels (*i.e.*, the ACX-K materials), characterized by basic surfaces (mean pH_{slurry} ~ 9.6), there is a decrease in the carbon content (from 75.2 % down to 69.3 %) in the order ACX-K1 > ACX-K2 > ACX-K4, accompanied by a parallel rise of oxygen content (from 22.7 to 28.6 %). This result shows that the increase of alkali content in the activation of RFX shields the carbonaceous material against excessive gasification and fixes more oxygen to the exposed carbon surface, which is also in accordance with the lower carbon yields obtained in the activation with KOH compared to the other activation procedures.

In opposition to the basic nature of the surface of ACX-K materials (pH_{slurry} from 9.4 up to 10.1, *cf*. Table 1), the parent RFX and ACX-P exhibit acidic surfaces, with slurry pH values of 4.0 and 3.7, respectively, and the ACX-S has a neutral surface character (pH_{slurry} = 7.2). Therefore, the activating agent affects the surface properties of the original resin. Thus, from the starting organic carbon xerogel (RFX), it is possible to derive purely neutral carbon gels, by simple carbonization or steam activation, acidic carbons, by activation with H_3PO_4, or basic carbons by activation with KOH. The importance of this derived property will depend on each particular application of these materials.

It is clear now that phosphorus atoms activate the acidic oxygen surface groups, while the K^+ ions help in the formation of basic oxygen groups during the activation process. FTIR spectra showed that ACX-P has phosphorous-containing groups on its surface, e.g. P=O, P–O–C, P=OOH, P–O–P and ionized P^+–O^- linkages in phosphate esters; similar results were obtained from activation of lignocellulosics with H_3PO_4 [25, 26]. It may be concluded that H_3PO_4 combines with organic species forming phosphate and polyphosphate bridges that connect biopolymer fragments. On the other hand, at 973 K, KOH can react with the polymeric gel, forming carbonates which are stable up to 1173 K. Oxygen functional groups on the resin surface can then react with K_2CO_3 and form intermediates like C–O–K. Then, the resulted groups further react with carbon of the precursor to produce K_2CO_3 and K_2O species. Thus, these surface functional groups can serve as active sites where chemical transformations occur via surface reactions [27] and the porous structure is developed. Moreover, the basic character may be associated with the presence of delocalized π electrons on the surface of the carbon gels due to their aromatic character and pyrone type structures [15]. As a conclusion, this work evidences that the chemical treatment can specify the type of oxygen functional groups on the carbon surface.

TABLE 1

3.2. Porosity development in ACXs

Table 2 shows the evaluated porosity characteristics of the synthesised materials. The parent organic xerogel (RFX) possesses a low total surface area (S_t^{α} =174 m^2 g^{-1}), but considerable total pore volume (V_P = 0.325 cm^3 g^{-1}) within meso-macroporosity (microporosity amounts only to 8 % of total porosity). Steam activation of RFX at 1073 K leads to a considerable generation of porosity in the organic resin (about 4-fold increase in S_t^{α} and about 1.5-fold in V_P), mostly within microporosity (63 % of total porosity). The porosity

attained by ACX-S approaches to those currently reported for some activated carbons, with respect to S_t^{α} and V_P. Impregnation with H_3PO_4, followed by pyrolysis at 773 K, causes a tremendous evolution in porosity, with a high yield of carbon (30.5 %, *cf*. Table 1). A high surface area carbon is thus obtained, with S_t^{α} of 1336 $m^2\ g^{-1}$ and V_P of 0.720 $cm^3\ g^{-1}$, mostly derived from micropores (89 %, *cf*. Table 2).

Alkali activation of the parent RFX with KOH at 973 K produces carbons with high surface area and advanced porosity. Successively regular promotion in the total surface area (S_t^{α}) and pore volume (V_P) is observed as the mass ratio of KOH/RFX increases from 1 to 4. The total surface area is raised from 991 $m^2\ g^{-1}$ to 1438 $m^2\ g^{-1}$ and pore volume from 0.606 $cm^3\ g^{-1}$ to 0.881 $cm^3\ g^{-1}$, respectively. Essentially microporous carbons are developed with contents in $S^{\alpha}_{mic}/S^{\alpha}_t$ and V^{α}_o/V_P ranging between 74 % to 88 % and 52 % to 77 %, respectively. However, a ratio of KOH/RFX = 2 seems to be the most effective to bring about particular generation of mesoporosity, namely to 26 % in S_t^{α} and 48 % in V_P. In general, the developed ACXs display porosity comparable to the typically high developed activated carbons derived from other source materials (coal, coconut shells and lignocellulosics). In particular, the action of KOH permeated through the primary particles promotes O-attachment with enhanced self-activation, generating thus intensive micropores with high S_t^{α} and V_P. In spite of the assumption that this process of self-activation is achieved at the consumption of O-functionalities, the KOH activation fixes and retains more oxygen than the other procedures (simple carbonization, steam or H_3PO_4-activation), as observed in Table 1.

Upon activation of RFX, the average pore width decreases (from 3.4 to 1.1 nm in the case of ACX-P), with generation of new micropores at the expense of mesopores. This may be attributed to the shrinkage effect during activation process.

As conclusion, highly porous carbon materials can be synthesised by evaporative drying in static flow of air followed by activation of resorcinol-formaldehyde xerogel under different conditions.

TABLE 2

3.3. Adsorption experiments

Adsorption experiments were carried out to evaluate the ability of the synthesised activated carbon xerogels to adsorb the selected model azo dyes. The results for the adsorption removal of C2R and OII, at the typical conditions referred in the experimental section, are given in Figure 2a and b, respectively.

The main observation evidenced from the results of both Figure 2a and b is that the activated carbon xerogels prepared by alkali activation with dry KOH at 973 K (ACX-K1, ACX-K2 and ACX-K4) are able to adsorb both azo dyes with a superior performance than the other materials. This superior adsorption capacity has already been mentioned in previous works on KOH activation of carbons [28]. Considering the cases of RFX, ACX-S and specially ACX-P, which presents the highest surface area and the greatest percentage of micropores among all tested materials, the removal of C2R and OII by adsorption is negligible, in spite of the slight removal in the case of OII with ACX-P. Taking into consideration that the ACX-P and the ACX-K materials are all characterized by high surface areas (*cf*. Table 2), it is possible to establish the surface chemistry as the key factor on the determination of the adsorption extent revealed by the tested xerogels, as observed for activated carbons in previous works [3, 4]. It is well known that a carbon surface may have both negatively and positively charged sites, depending on the solution pH. At some pH – the point of zero charge (*PZC*) – the overall surface charge will be zero, but for pH values below the *PZC*, the surface will be covered by protonated groups, thus attracting anions [29, 30].

Considering the chemical properties of the synthesised activated carbon xerogels (*cf*. Table 1), it is possible to realize that the ACX-K materials presents strong basic character, which translates into higher *PZC* values compared with the other tested materials. The experiments were performed at pH = 3, *i.e*. in acidic media, favouring thereby, as previously stated, the interaction between the carbon materials surface and the anionic dyes. Therefore, it seems possible to establish a relation between the superior adsorption performances achieved by the ACX-K materials and their surface chemical properties, *i.e*., with their strong basic character.

Comparing the adsorption removals of C2R and OII, it is observed that, with the exception of RFX and ACX-S, which reveal a negligible adsorption removal for both dyes, all the other synthesised activated carbon xerogels are able to remove in general larger amounts of OII than C2R. These differences may be related with the OII molecules, which are characterized by a lower molecular weight and a less ramified chemical structure, allowing a better accessibility to the micropores of the adsorbents. In addition, analysing more in detail the results obtained with the ACX-K materials, it is observed that the adsorption removal extent achieved with ACX-K1 is almost independent of the adsorbate considered, since the removal extent of OII slightly increases 0.1 %, compared to the removal of C2R. However, for ACX-K2 and ACX-K4, which present higher surface areas (*cf*. Table 2), the increment is more visible.

FIGURE 2

The adsorption removals of both azo dyes obtained with the synthesised carbon xerogels after 150 min at 303 K and pH = 3 are given in Table 3, in terms of adsorbent mass and surface area, and in dye removal percentage. These results confirm the high adsorption performance achieved by the ACX-K materials for both dyes (from over 215 mg g^{-1}, concerning the adsorption removal of C2R on ACX-K2, up to 499 mg g^{-1}, in the case of the

adsorption removal of OII on ACX-K4). In addition, the values for the adsorption removal of C2R and OII per surface area of adsorbent (Table 3) are extensively different for each one, even for materials with similar textural properties, confirming that the performances of the adsorbents are mainly determined by its surface chemical interactions with the dyes, rather than with its textural properties. As an example, the total surface area (S^{α}_{t}) of ACX-P is 1336 $m^2\ g^{-1}$ (*cf*. Table 2), a value between 1052 $m^2\ g^{-1}$ and 1438 $m^2\ g^{-1}$, the total surface areas of ACX-K2 and ACX-K4, respectively. However, the adsorption removals of C2R and OII are considerably higher when using any of these last two materials (*cf*. Table 3) than the adsorption removal obtained with the ACX-P. This is in accordance to the differences observed between the values of the removals in terms of specific area.

3.3.1. Effect of temperature

Since the synthesised activated carbon xerogels have revealed interesting adsorption characteristics, further studies were carried out to explore their properties and the effect of temperature on their performance. In that sense, experiments with C2R were performed at the previously referred conditions, except the temperature, which was increased from 303 K up to 323 K. The removals of C2R by adsorption obtained by the synthesised activated carbon xerogels at both temperatures are given in Table 3.

In general, temperature increment reveals a negative effect, as it leads to a slight decrease on adsorption removal (*cf*. Table 3). This behaviour was expected, considering that adsorption processes usually are exothermic [31]. ACX-S and ACX-K2 were exceptions, given that the adsorption of C2R slightly increases as the temperature goes from 303 K up to 323 K. This may suggest an endothermic nature of the adsorption in these cases, an unusual behaviour that

several authors have reported concerning the adsorption of different dyes on different types of adsorbents [32-34].

TABLE 3

3.3.2. Effect of adsorbent mass

To assess the ability of the synthesised activated carbon xerogels to promote the complete dye removal by adsorption, some experiments with increased adsorbent mass were also performed. The C2R was selected due to its lower removal at the conditions initially tested (*cf*. Figure 2). The mass of the tested materials was increased to 0.5 g L^{-1}, considering $T = 323$ K and pH = 3. The removals of C2R by adsorption after 150 min with different adsorbent mass are given in Table 3.

From Table 3 it is observed that ACX-K4 is able to completely remove the C2R content by adsorption, considering an adsorbent mass of 0.5 g L^{-1}, and that, in the case of ACX-K1 and ACX-K2, adsorption removals of over 97 % of the C2R content are obtained. It is also possible to realise that, at these conditions, all the tested materials are able to adsorb the dye, even in the case of RFX and ACX-S, where the adsorption observed is still very low.

Analysing the results gathered in Table 3, it is possible to observe that for most of the ACXs, and at the same temperature (323 K), the dye removal decreases with the increase of the mass of adsorbent in terms of their specific surface area (μg m^{-2}). Previous results in the literature with granular activated carbon and natural zeolite concluded that the solid diffusivity varies with the variation of the adsorbent mass, specifically, it decreases with increasing adsorbent mass [35]. For the same initial dye concentration and for increasing adsorbent mass, it is expected an increase in the slope of the adsorption isotherm at the final equilibrium concentration and a decrease on the surface coverage [36], as well as in the solid

diffusion coefficient [35]. This is in agreement with our results. On the other hand, for RFX and ACX-P, the surface coverage increases as their mass increases, suggesting the existence of other mechanisms involved in the adsorption process. The fully understanding of these mechanisms is not an objective of the present work, so further studies were not performed.

3.3.3. Adsorption dynamics

A simple evaluation of the adsorption dynamics was performed for the synthesised activated carbon xerogels that have revealed higher adsorption activity, *i.e.*, the ACX-K materials. The constants of the Ho and McKay's pseudo second order kinetics [24], obtained for the adsorption of C2R considering different temperatures and a catalyst load of 0.1 g L^{-1}, are given in Table 4. From the high correlation coefficients (r^2) obtained and also shown in Table 5, it is possible to conclude that the kinetic model used is able to accurately adjust the experimental data. The curves shown in Figure 2, as well as dynamic data in linear coordinates (t/q_t against t) shown in Figure 3, prove the validity of the pseudo second order model used to fit experimental data.

TABLE 4

Comparing the calculated q_e (number of active sites) values produced by the model (Table 4) with the measured adsorption removal amounts (Table 3) for the same materials at the same conditions (initial concentration of 0.1 g L^{-1}) there is a visible correlation. The chosen model is therefore well suited for this system and confirms the fact that q_e should reflect the changes on the nature of the adsorbent. The ACX-K4 is obviously a better adsorbent with almost the double of the capacity of the parent xerogels activated with lower KOH masses.

On the other hand, given the predictive value of the model, is worth noticing that only 60 min are needed to attain 95 % of the total adsorption removal (Figure 2).

FIGURE 3

3.4. CWPO experiments

The synthesised activated carbon xerogels were also tested in the CWPO of C2R and OII, at the typical conditions referred in the experimental section. The results are given in Figure 4a and b, respectively.

First, it is important to notice from Figure 4a and b that the introduction of H_2O_2 leads to partial removal of C2R and OII in all the performed experiments and that the performance of the ACX-K materials is largely superior to the performance of the other materials in terms of the removal of both dyes by CWPO, as also previously observed in the adsorption experiments. Comparing the concentration decay curves obtained for the CWPO removal of both dyes, it is observed that all the tested materials present higher performance in the case of C2R. This is in the opposite trend to what was observed in the adsorption experiments, where higher removals were obtained with OII. This observation suggests that C2R is more prone to oxidation than OII. However, as referred in section 2.5.2, the same concentration of H_2O_2 was used in all CWPO experiments, resulting in different molar ratios between the oxidizing agent and the dyes. Therefore, it is not possible to draw a definitive conclusion on this matter, but a possible explanation may be related with the less ramified structure of OII molecules, which may hinder the attack on their chemical bonds.

It is also observed from Figure 4a and b that the CWPO removal of C2R promoted by ACX-K1 is higher than the promoted by ACX-K2, however the opposite situation is found when the azo dye OII is used. This is mainly a result of the different contributions of adsorption presented by these materials, as previously mentioned and discussed.

FIGURE 4

For comparison purposes, the adsorption and CWPO removals of both azo dyes after 150 min, considering T = 303 K, are given in Figure 5a and b. The superior performance of the ACX-Ks compared to the other tested materials is well evidenced, in particular for the removal of C2R. The removals of both azo dyes in the CWPO experiments are considered marginal when using the RFX, ACX-S and ACX-P materials. When using the ACX-K1, ACX-K2 and ACX-K4, the C2R removals by CWPO increases 33 %, 24 % and 20 %, respectively, compared with the removals observed in the adsorption experiments. In the case of OII and considering the same order, the increases observed are 7 %, 4 % and 4 %. Blank experiments performed at the same operating conditions have revealed that the non-catalytic oxidation of OII and C2R promoted by H_2O_2 (34.6 mmol L^{-1}) is around 1 % for OII and 10 % for C2R, indicating that the synthesised activated carbon xerogels, specially the ACX-Ks, are catalytic active materials for the CWPO of azo dyes. Further, the differences observed in the CWPO experiments between the different ACX-K materials attest their own influence on the azo dyes oxidation, which may be mainly due to the formation of $OH^{\bullet}$ radicals from H_2O_2 decomposition over their surface. Other authors concluded that the surface composition of activated carbons plays an important role on H_2O_2 decomposition, being activated carbons of basic character more active for the formation of $OH^{\bullet}$ radicals than acid ones [5, 37, 38], which is in agreement with our findings.

The order obtained for the catalytically active ACX-Ks was ACX-K1 > ACX-K2 > ACX-K4, but the opposite order was found regarding to the oxygen content (*cf.* Table 1). Thus, this suggests that the presence of surface oxygen groups reduces the catalytic activity of carbons with similar structure, which is in accordance with other authors findings on activated carbons [39].

FIGURE 5

3.4.1. Effect of temperature

As in the adsorption experiments, the effect of temperature on C2R removal by CWPO was also evaluated, considering the ACX-K materials. The operating temperature was increased from 303 K to 323 K, maintaining the remaining parameters constant. The removals of C2R are given in Table 5.

It is observed from Table 5 that the removal of C2R by CWPO increases for all the ACX-K materials, as a consequence of increasing the temperature from 303 K to 323 K. This is a direct consequence of higher reaction rate between H_2O_2 and the catalysts, which is in accordance with H_2O_2 decomposition tests performed at both temperatures. Comparing the results obtained in the CWPO experiments at 323 K with the results obtained in the adsorption experiments at the same temperature, it is found that the CWPO removals achieved with the ACX-K materials increases when increasing the temperature from 303 K to 323 K. When using the ACX-K1, ACX-K2 and ACX-K4, the C2R removals by CWPO increases 67 %, 59 % and 49 %, respectively, compared with the removals observed in the adsorption experiments.

Table 5 presents the overall results obtained for the azo dyes removal by CWPO, at different conditions. By comparison with the results from adsorption at T = 303 K (*cf*. Table 3), it is possible to verify that the CWPO process enhances the removal of C2R from over 215 mg g^{-1}, concerning to the adsorption removal of C2R on ACX-K2, up to 448 mg g^{-1} and from 499 mg g^{-1}, in the case of the adsorption removal of OII on ACX-K4, up to 524 mg g^{-1}. Likewise, considering T = 323 K (*cf*. Table 3 and Table 5), it is observed that the enhancement by CWPO is even greater. The C2R removals by adsorption were near 214 mg g^{-1}, 242 mg g^{-1} and 411 mg g^{-1}, for ACX-K1, ACX-K2 and ACX-K4, respectively, while by CWPO, values near 855 mg g^{-1}, 815 mg g^{-1} and 875 mg g^{-1} were achieved.

TABLE 5

3.4.2. Reusability cycles

Experiments using the xerogel with highest catalytic activity (ACX-K1) were performed in a series of three consecutive CWPO runs at the optimal operating temperature (323 K). After each run, the catalyst was filtered, washed and dried at 333 K overnight, and then reused with a fresh C2R solution. The aim was to assess the catalyst stability in CWPO, a basic requirement for its application at industrial scale.

C2R concentration decay curves obtained in this series of experiments are given in Figure 6. As expected, the removal of C2R is faster in the first run when compared to the second, due to the contribution of adsorption in the first use of the catalyst. In addition, the difference observed is consistent with the results obtained for the removal of C2R by adsorption on ACX-K1, as listed in Table 3. This phenomenon, plus the fact that, once saturated, the ACX-K1 is able to remove 71% of C2R by CWPO after 150 min of reaction, puts in evidence its catalytic activity for this process. Comparing the concentration decay curves obtained for the second and third runs, it is observed that they are practically identical, indicating catalyst stability. In addition, ACX-K1 is found as promising as other metal-free catalysts [3, 4, 22, 40] and Fe-based catalysts reported in literature for the removal of C2R and OII by CWPO in comparable conditions. For possible industrial applications, the prepared material should be subjected to further studies, including experiments with real case effluents to explore the CWPO process ability to meet EU and US directives.

FIGURE 6

4. Conclusions

Highly porous carbon materials (activated carbon xerogels), with distinct surface chemistries, can be synthesised by polymerization/polycondensation reactions followed by activation of the resultant resorcinol-formaldehyde xerogel under different conditions.

Adsorption of anionic azo dyes (Chromotrope 2R – C2R, and Orange II – OII) revealed that the materials produced by activation with KOH (ACX-K) have superior adsorption performances compared to the other synthesised materials, explained by the strong basic character of ACX-K materials, which enhances the interaction between the basic carbon materials surface and the anionic dyes. After 150 min of adsorption and considering T = 303 K, pH = 3 and adsorbent mass = 0.1 g L^{-1}, the ACX-K materials exhibit adsorption performances from over 215 mg g^{-1}, concerning to the adsorption removal of C2R on ACX-K2, up to 499 mg g^{-1}, in the case of the adsorption removal of OII on ACX-K4.

In an attempt to maximize the removal of C2R by pure adsorption, it was found that the ACX-K4 is able to completely remove the azo dye content after 150 min of adsorption, considering an adsorbent load of 0.5 g L^{-1}, T = 323 K and pH =3. In the case of ACX-K1 and ACX-K2, under the same conditions, adsorption removals over than 97 % of the C2R content are obtained.

CWPO experiments show that the ACX-K materials possess catalytic activity for the oxidation of azo dyes, enhancing the removals of C2R and OII, compared to the removals observed by adsorption. When using ACX-K1, ACX-K2 and ACX-K4, the C2R removals by CWPO at 323 K increases 67 %, 59 % and 49 %, respectively, compared with the removals observed in the adsorption experiments performed at the same conditions. The order of catalytic activity found for the ACX-K catalysts is in the opposite order of their oxygen content, what allows concluding that the catalytic activity of the ACX-K materials increases

with the decrease of surface oxygen groups. Recycling studies with ACX-K1 show that this catalyst is also very stable in CWPO, indicating that alkali activation of carbon xerogels with dry KOH is a promising route to produce active and stable catalysts for CWPO.

Acknowledgements

Work supported by project PTDC/AAC-AMB/110088/2009 and partially by project PEst-C/EQB/LA0020/2011, financed by FEDER through COMPETE - Programa Operacional Factores de Competitividade and by FCT - Fundação para a Ciência e a Tecnologia. AMTS acknowledges financial support from POCI/N010/2006.

References

[1] A. Rey, A. Bahamonde, J.A. Casas, J.J. Rodríguez, Selectivity of hydrogen peroxide decomposition towards hydroxyl radicals in catalytic wet peroxide oxidation (CWPO) over Fe/AC catalysts, Water Science and Technology, 61 (2010) 2769-2778.

[2] A. Dhaouadi, N. Adhoum, Heterogeneous catalytic wet peroxide oxidation of paraquat in the presence of modified activated carbon, Applied Catalysis B: Environmental, 97 (2010) 227-235.

[3] H.T. Gomes, S.M. Miranda, M.J. Sampaio, J.L. Figueiredo, A.M.T. Silva, J.L. Faria, The role of activated carbons functionalized with thiol and sulfonic acid groups in catalytic wet peroxide oxidation, Applied Catalysis B: Environmental, 106 (2011) 390-397.

[4] H.T. Gomes, S.M. Miranda, M.J. Sampaio, A.M.T. Silva, J.L. Faria, Activated carbons treated with sulphuric acid: Catalysts for catalytic wet peroxide oxidation, Catalysis Today, 151 (2010) 153-158.

[5] F. Lücking, H. Köser, M. Jank, A. Ritter, Iron powder, graphite and activated carbon as catalysts for the oxidation of 4-chlorophenol with hydrogen peroxide in aqueous solution, Water Research, 32 (1998) 2607-2614.

[6] R.W. Pekala, Organic aerogels from the polycondensation of resorcinol with formaldehyde, Journal of Materials Science, 24 (1989) 3221-3227.

[7] E.J. Zanto, S.A. Al-Muhtaseb, J.A. Ritter, Sol-gel-derived carbon aerogels and xerogels: Design of experiments approach to materials synthesis, Industrial & Engineering Chemistry Research, 41 (2002) 3151-3162.

[8] S.A. Al-Muhtaseb, J.A. Ritter, Preparation and properties of resorcinol-formaldehyde organic and carbon gels, Advanced Materials, 15 (2003) 101-114.

[9] N. Job, R. Pirard, J. Marien, J.P. Pirard, Porous carbon xerogels with texture tailored by pH control during sol-gel process, Carbon, 42 (2004) 619-628.

[10] K. Kadirvelu, J. Goel, C. Rajagopal, Sorption of lead, mercury and cadmium ions in multi-component system using carbon aerogel as adsorbent, Journal of Hazardous Materials, 153 (2008) 502-507.

[11] B.S. Girgis, A.A. Attia, N.A. Fathy, Potential of nano-carbon xerogels in the remediation of dye-contaminated water discharges, Desalination, 265 (2011) 169-176.

[12] C. Moreno-Castilla, F.J. Maldonado-Hódar, Carbon aerogels for catalysis applications: An overview, Carbon, 43 (2005) 455-465.

[13] E. Frackowiak, F. Beguin, Carbon materials for the electrochemical storage of energy in capacitors, Carbon, 39 (2001) 937-950.

[14] N. Job, B. Heinrichs, S. Lambert, J.-P. Pirard, J.-F. Colomer, B. Vertruyen, J. Marien, Carbon xerogels as catalyst supports: Study of mass transfer, AIChE Journal, 52 (2006) 2663-2676.

[15] L. Zubizarreta, A. Arenillas, J.-P. Pirard, J.J. Pis, N. Job, Tailoring the textural properties of activated carbon xerogels by chemical activation with KOH, Microporous and Mesoporous Materials, 115 (2008) 480-490.

[16] M.S. Contreras, C.A. Paez, L. Zubizarreta, A. Leonard, S. Blather, C.G. Olivera-Fuentes, A. Arenillas, J.-P. Pirard, N. Job, A comparison of physical activation of carbon xerogels with carbon dioxide with chemical activation using hydroxides, Carbon, 48 (2010) 3157-3168.

[17] C.J. Gommes, N. Job, J.-P. Pirard, S. Blacher, B. Goderis, Critical opalescence points to thermodynamic instability: Relevance to small-angle X-ray scattering of resorcinol-formaldehyde gel formation at low pH, Journal of Applied Crystallography, 41 (2008) 663-668.

[18] N. Job, S. Berthon-Fabry, M. Chatenet, J. Marie, M. Brigaudet, J.-P. Pirard, Nanostructured carbons as platinum catalyst supports for proton exchange membrane fuel cell electrodes, Topics in Catalysis, 52 (2009) 2117-2122.

[19] T. Yamamoto, T. Sugimoto, T. Suzuki, S.R. Mukai, H. Tamon, Preparation and characterization of carbon cryogel microspheres, Carbon, 40 (2002) 1345-1351.

[20] N.A. Fathy, Preparation and characterization of carbon xerogels prepared from polycondensation of resorcinol with formaldehyde, Ph.D. Thesis, Ain-Shams University, Cairo, Egypt, 2010.

[21] M.J. Sellez-Perez, J.M. Martin-Martinez, Classification of αs plots obtained from N_2/77 K adsorption isotherms of activated carbons, Fuel, 70 (1991) 877-881.

[22] F. Duarte, F.J. Maldonado-Hódar, L.M. Madeira, Influence of the characteristics of carbon materials on their behaviour as heterogeneous Fenton catalysts for the elimination of the azo dye Orange II from aqueous solutions, Applied Catalysis B: Environmental, 103 (2011) 109-115.

[23] V. Alexéev, Quantitative analysis, 3rd ed. (portuguese edition), Lopes da Silva Editora, Porto, 1983.

[24] Y.S. Ho, G. McKay, The kinetics of sorption of divalent metal ions onto sphagnum moss peat, Water Research, 34 (2000) 735-742.

[25] A.M. Puziy, O.I. Poddubnaya, A. Martínez-Alonso, A. Castro-Muñiz, F. Suárez-García, J.M.D. Tascón, Oxygen and phosphorus enriched carbons from lignocellulosic material, Carbon, 45 (2007) 1941-1950.

[26] A.M. Puziy, O.I. Poddubnaya, A. Martínez-Alonso, F. Suárez-García, J.M.D. Tascón, Synthetic carbons activated with phosphoric acid: I. Surface chemistry and ion binding properties, Carbon, 40 (2002) 1493-1505.

[27] L. Chunlan, X. Shaoping, G. Yixiong, L. Shuqin, L. Changhou, Effect of pre-carbonization of petroleum cokes on chemical activation process with KOH, Carbon, 43 (2005) 2295-2301.

[28] F.C. Wu, R.L. Tseng, R.S. Juang, Preparation of highly microporous carbons from fir wood by KOH activation for adsorption of dyes and phenols from water, Separation and Purification Technology, 47 (2005) 10-19.

[29] F. Rodríguez-Reinoso, The role of carbon materials in heterogeneous catalysis, Carbon, 36 (1998) 159-175.

[30] Y. Al-Degs, M.A.M. Khraisheh, S.J. Allen, M.N. Ahmad, Effect of carbon surface chemistry on the removal of reactive dyes from textile effluent, Water Research, 34 (2000) 927-935.

[31] Y.S. Al-Degs, M.I. El-Barghouthi, A.H. El-Sheikh, G.A. Walker, Effect of solution pH, ionic strength, and temperature on adsorption behavior of reactive dyes on activated carbon, Dyes and Pigments, 77 (2008) 16-23.

[32] A.R. Cestari, E.F.S. Vieira, A.G.P. dos Santos, J.A. Mota, V.P. de Almeida, Adsorption of anionic dyes on chitosan beads. 1. The influence of the chemical structures of dyes and temperature on the adsorption kinetics, Journal of Colloid and Interface Science, 280 (2004) 380-386.

[33] S. Netpradit, P. Thiravetyan, S. Towprayoon, Adsorption of three azo reactive dyes by metal hydroxide sludge: Effect of temperature, pH, and electrolytes, Journal of Colloid and Interface Science, 270 (2004) 255-261.

[34] Y. Guo, J. Zhao, H. Zhang, S. Yang, J. Qi, Z. Wang, H. Xu, Use of rice husk-based porous carbon for adsorption of Rhodamine B from aqueous solutions, Dyes and Pigments, 66 (2005) 123-128.

[35] V. Meshko, L. Markovska, M. Mincheva, A.E. Rodrigues, Adsorption of basic dyes on granular acivated carbon and natural zeolite, Water Research, 35 (2001) 3357-3366.

[36] V. Meshko, L. Markovska, M. Mincheva, Two resistance mass transfer model for the adsorption of basic dyes from aqueous solutions on natural zeolite, Bull. Chem. Technol. Macedonia, 18 (1999) 161-169.

[37] L.B. Khalil, B.S. Girgis, T.A.M. Tawfik, Decomposition of H_2O_2 on activated carbon obtained from olive stones, Journal of Chemical Technology & Biotechnology, 76 (2001) 1132-1140.

[38] V.P. Santos, M.F.R. Pereira, P.C.C. Faria, J.J.M. Órfão, Decolourisation of dye solutions by oxidation with H_2O_2 in the presence of modified activated carbons, Journal of Hazardous Materials, 162 (2009) 736-742.

[39] A. Rey, J.A. Zazo, J.A. Casas, A. Bahamonde, J.J. Rodríguez, Influence of the structural and surface characteristics of activated carbon on the catalytic decomposition of hydrogen peroxide, Applied Catalysis A: General, 402 (2011) 146-155.

[40] J.H. Ramirez, F.J. Maldonado-Hódar, A.F. Pérez-Cadenas, C. Moreno-Castilla, C.A. Costa, L.M. Madeira, Azo-dye Orange II degradation by heterogeneous Fenton-like reaction using carbon-Fe catalysts, Applied Catalysis B: Environmental, 75 (2007) 312-323.

TABLES

Table 1. Carbon yield, slurry pH (pH_{slurry}) and elemental chemical analysis of the synthesised activated carbon xerogels and their RFX parent.

Material	Carbon yield	pH_{slurry}	% C	% H	% O	C_{at}^{*}	H_{at}^{*}	O_{at}^{*}	H/C	O/C
RFX	-	4.0	58.4	4.7	36.9	4.9	4.7	2.3	0.97	0.47
ACX-S	21.0	7.2	77.1	3.2	19.7	6.4	3.2	1.2	0.50	0.19
ACX-P	30.5	3.7	83.3	3.3	13.4	6.9	3.3	0.8	0.48	0.12
ACX-K1	11.0	10.1	75.2	2.3	22.7	6.3	2.3	1.4	0.37	0.23
ACX-K2	12.5	9.4	71.2	2.4	26.6	5.9	2.4	1.7	0.41	0.28
ACX-K4	20.6	9.4	69.3	2.1	28.6	5.8	2.1	1.8	0.37	0.31

*Refers to atomic content of either component.

Table 2. Textural properties of the synthesised activated carbon xerogels and their RFX parent.

Material	S_{BET}/ ($m^2\ g^{-1}$)	S^{α}_{t}/ ($m^2\ g^{-1}$)	S^{α}_{n}/ ($m^2\ g^{-1}$)	S^{α}_{mic}/ ($m^2\ g^{-1}$)	R_p/ nm	V^{α}_{o}/ ($cm^3\ g^{-1}$)	V_P/ ($cm^3\ g^{-1}$)	V^{α}_{o}/ V_P	S^{α}_{mic}/ S^{α}_{t}
RFX	194	174	160	14	3.4	0.025	0.325	0.08	0.08
ACX-S	669	653	146	507	1.4	0.291	0.464	0.63	0.78
ACX-P	1318	1336	48	1288	1.1	0.643	0.720	0.89	0.96
ACX-K1	916	991	121	870	1.3	0.433	0.606	0.71	0.88
ACX-K2	1051	1052	273	779	1.5	0.396	0.761	0.52	0.74
ACX-K4	1438	1438	190	1248	1.2	0.680	0.881	0.77	0.87

Table 3. Adsorption removal of C2R and OII obtained with the synthesised activated carbon xerogels and their RFX parent after 150 min at pH = 3 and different temperatures and adsorbent mass.

$C_{Material}$	Temperature	Pollutant	Removal*	Material					
				RFX	ACX-S	ACX-P	ACX-K1	ACX-K2	ACX-K4
0.1 g L^{-1}	303 K	C2R	%	0	0	1	26	22	43
			mg g^{-1}	0.6	0.1	8.9	264.0	215.4	424.6
			µg m^{-2}	3.2	0.2	6.7	288.2	205.0	295.2
		OII	%	0	0	6	27	31	49
			mg g^{-1}	0.5	0.0	58.9	269.4	315.7	499.1
			µg m^{-2}	2.6	0.0	44.7	294.1	300.4	347.1
	323 K	C2R	%	0	1	0	22	24	41
			mg g^{-1}	0.0	8.1	0.0	213.5	242.0	410.8
			µg m^{-2}	0.0	12.0	0.0	233.0	230.2	285.7
0.5 g L^{-1}	323 K	C2R	%	1	2	10	98	97	100
			mg g^{-1}	2.9	4.4	20.2	196.6	193.8	200.2
			µg m^{-2}	14.9	6.6	15.3	214.6	184.4	139.2

*Maximum error is 2 %, considering 99 % certainty.

Table 4. Constants of Ho and McKay's pseudo second order kinetics, obtained for the adsorption of C2R with the synthesised ACX-K materials, considering T = 303 K and T = 323 K, for a catalyst load of 0.1 g L^{-1} and pH = 3. k_{PSO} is the rate constant of adsorption, q_e is the amount of dye adsorbed at equilibrium (*i.e.*, the number of active sites) and r^2 is the correlation coefficient of the linear fitting.

Temperature	Parameter	Material		
		ACX-K1	ACX-K2	ACX-K4
303 K	q_e/ mg g^{-1}	278	222	455
	$k_{PSO}x10^5$/ g mg^{-1} min^{-1}	36	127	25
	r^2	0.998	0.9998	0.9995
323 K	q_e/ mg g^{-1}	227	244	417
	$k_{PSO}x10^5$/ g mg^{-1} min^{-1}	48	142	48
	r^2	0.999	0.9997	0.9999

Table 5. CWPO removal of the C2R and OII obtained by the synthesised ACX-K materials (0.1 g L^{-1}) after 150 min at different temperatures, H_2O_2 concentration of 34.6 mmol L^{-1} and pH = 3.

Temperature	Pollutant	Removal*	Material		
			ACX-K1	ACX-K2	ACX-K4
303 K	C2R	%	60	46	62
		mg g^{-1}	580.3	447.5	612.2
		µg m^{-2}	633.6	425.8	425.7
	OII	%	34	35	53
		mg g^{-1}	336.4	345.2	524.0
		µg m^{-2}	367.2	328.4	364.4
323 K	C2R	%	88	83	90
		mg g^{-1}	855.0	814.8	874.9
		µg m^{-2}	933.4	775.3	608.4

*Maximum error is 2 %, considering 99 % certainty.

FIGURE CAPTIONS

Figure 1. Molecular structure of Chromotrope 2R (a) and Orange II (b).

Figure 2. Concentration decay curves obtained for the adsorption removal of C2R (a) and OII (b) using the synthesised activated carbon xerogels and their RFX parent (0.1 g L^{-1}), considering T = 303 K and pH = 3.

Figure 3. Kinetic data in linear coordinates, according to Ho and McKay's pseudo second order model as given in eq. 2. Points represent experimental data, while lines represent the kinetic model.

Figure 4. Concentration decay curves obtained for the CWPO removal of C2R (a) and OII (b) using the synthesised activated carbon xerogels and their RFX parent (0.1 g L^{-1}) and H_2O_2 (34.6 mmol L^{-1}). Experiments considering T = 303 K and pH = 3.

Figure 5. C2R (a) and OII (b) removal obtained in the adsorption and CWPO experiments, after 150 min, considering T = 303 K, pH = 3 and H_2O_2 concentration of 34.6 mmol L^{-1} (in the CWPO experiments).

Figure 6. Concentration decay curves obtained for the CWPO removal of C2R, in a series of three runs, by consecutive reuse of the synthesised activated carbon xerogel ACX-K1 (0.1 g L^{-1}) and H_2O_2 (34.6 mmol L^{-1}). Experiments considering T = 323 K and pH = 3.

FIGURE 1

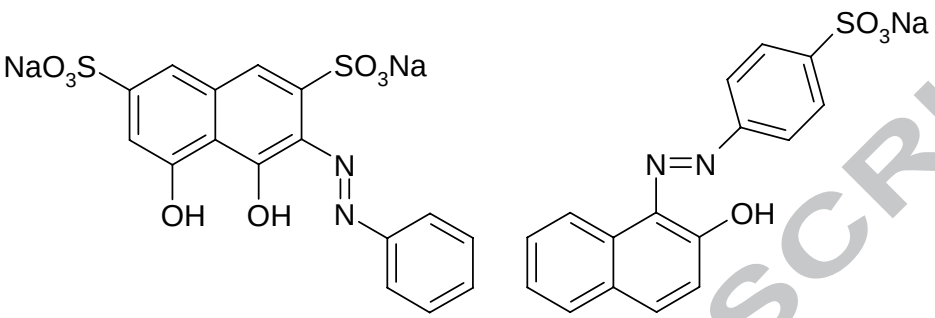

FIGURE 2

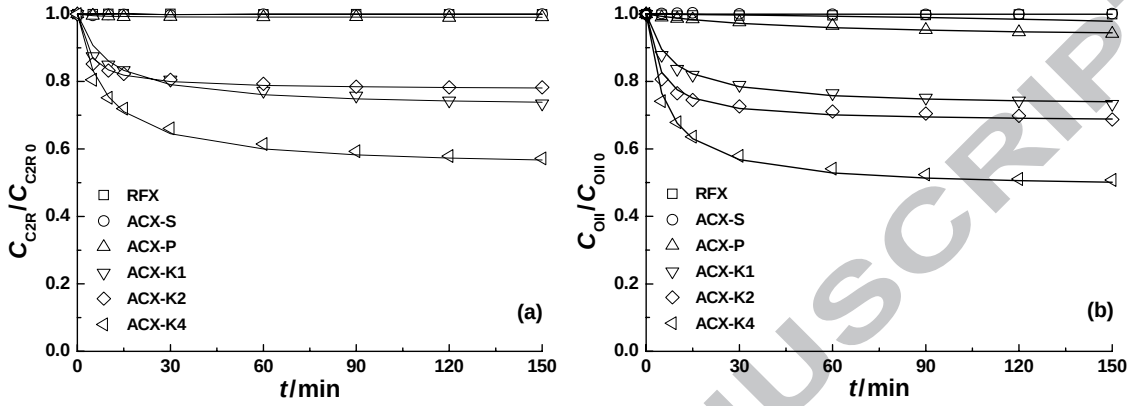

FIGURE 3

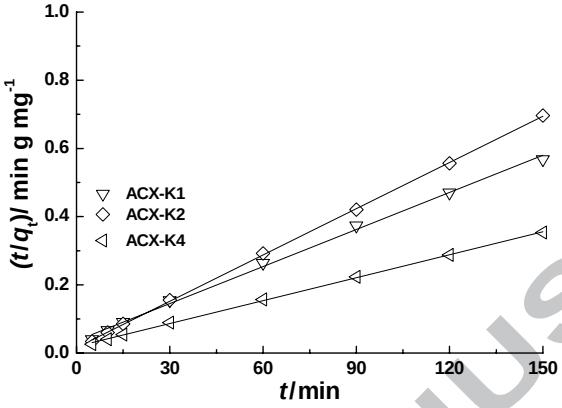

FIGURE 4

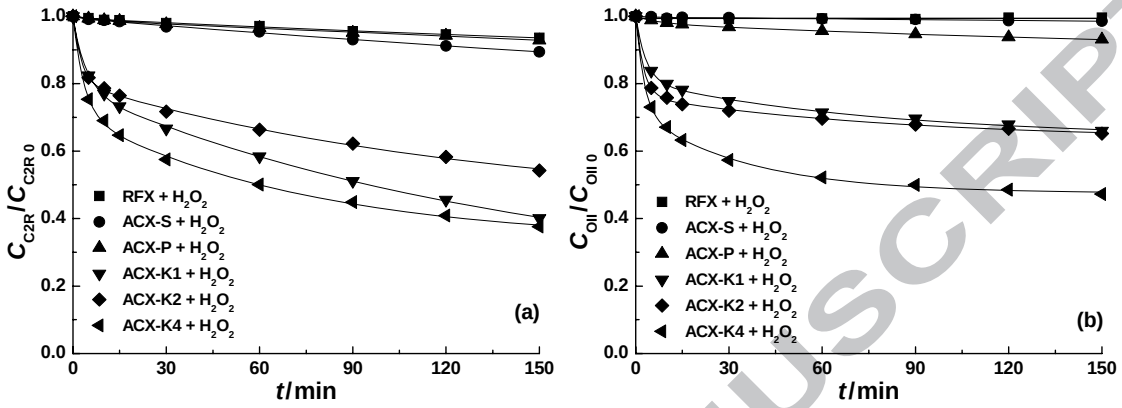

FIGURE 5

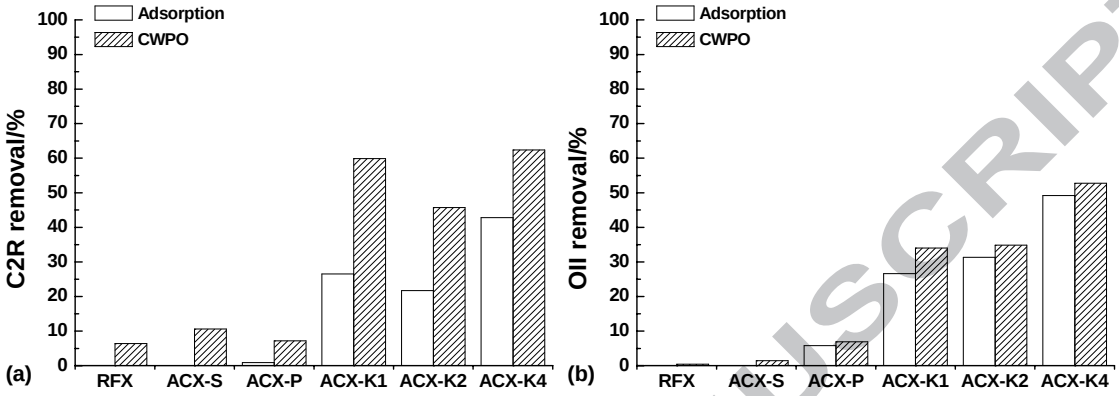

FIGURE 6

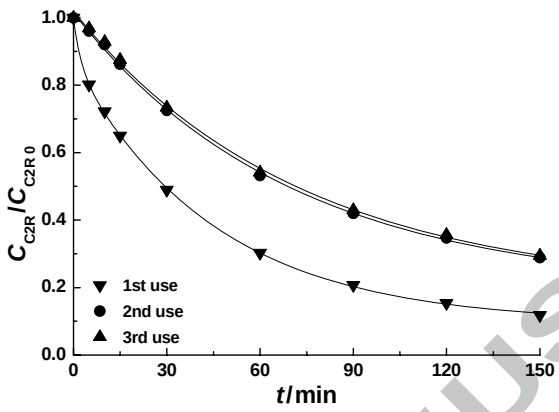

- Activated carbon xerogels are produced by activation of an organic xerogel.
- Different activation procedures: steam, activation with H_3PO_4 and with dry KOH.
- Materials with higher basicity exhibit higher adsorption performances.
- Materials with higher basicity possess significant catalytic activity for oxidation.
- Complete removal of the pollutants is obtained with optimized operating conditions.